ELSEVIER

Coordination Chemistry Reviews 229 (2002) 123–132

COORDINATION CHEMISTRY REVIEWS

www.elsevier.com/locate/ccr

Luminescence studies of dinuclear platinum(II) alkynyl complexes and their mixed-metal platinum(II)–copper(I) and –silver(I) complexes

Keith Man-Chung Wong, Chi-Kuen Hui, Ka-Lai Yu, Vivian Wing-Wah Yam *

Department of Chemistry, The University of Hong Kong, Pokfulam Road, Hong Kong, People's Republic of China

Received 27 November 2001; accepted 28 March 2002

Contents

Abstract

Two series of dinuclear platinum(II) alkynyl complexes, $[Pt_2(\mu\text{-dppm})_2(\mu\text{-C}{\equiv}CR)(C{\equiv}CR)_2]^+$ (in A-frame structure) and $[Pt_2(\mu\text{-dppm})_2(C{\equiv}CR)_4]$ (in face-to-face structure), were synthesized and characterized. All of them exhibit rich photoluminescence in degassed solutions and in the solid-state. Their emissions were assigned as derived from states of triplet metal–metal bond-to-ligand charge transfer (^{3}MMLCT) origin. The effects of the variation of alkynyl substituents and Pt···Pt bond distances on their photophysical behaviours have been studied. Resonance Raman (RR) spectroscopic experiments supported the spectral assignments and variable-temperature NMR studies showed the fluxional properties of the A-frame complexes. Encapsulation of copper(I) or silver(I) ion in between the two alkynyl groups in one of the face-to-face complexes $[Pt_2(\mu\text{-dppm})_2(C{\equiv}CPh)_4]$, via π-coordination was found to vary its luminescence properties. © 2002 Elsevier Science B.V. All rights reserved.

Keywords: Platinum(II); Alkynyl; π-Coordination; Pt···Pt interaction; Luminescence; MMLCT

1. Introduction

Square-planar platinum(II) complexes are well known to exhibit metal···metal interactions. There are a number of unique spectroscopic features associated with these metal···metal interactions and some of them even show rich polymorphism. For example, $[Pt(bpy)Cl_2]$ is known to exist in two forms, a yellow form that shows a Pt···Pt separation of 4.44 Å while the red form has a Pt···Pt distance of 3.45 Å [1,2]. Metal···metal separation seems to play an important role in governing the spectroscopic behaviour of these compounds. One approach to probe the role of metal···metal interaction in determining the spectroscopic properties of these d^8 square-planar complexes involves

---

* Corresponding author. Tel.: +852-2859-2153; fax: +852-2857-1586

E-mail address: wwyam@hku.hk (V.W.-W. Yam).

PII: S0010-8545(02)00104-2

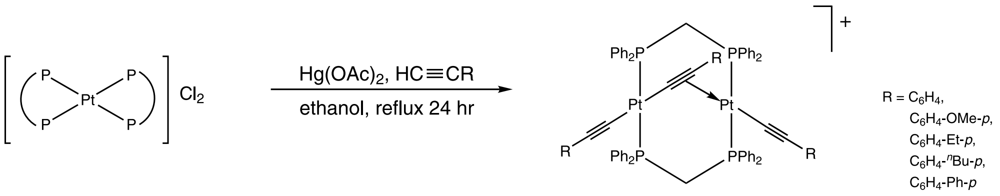

Scheme 1.

the design and synthesis of discrete molecules with known metal···metal distances. This approach has been adopted in the study of the well known dinuclear platinum(II) complex, $[Pt_2(POP)_4]^{4-}$, which has been shown to exhibit rich luminescence and photochemistry associated with the presence of Pt···Pt interaction [3]. As an extension of our recent work on the photoluminescence studies of transition metal–alkynyl complexes [4–7], a programme was launched to investigate the dinuclear platinum(II) alkynyl systems, $[Pt_2(\mu\text{-dppm})_2(\mu\text{-C}{\equiv}CR)(C{\equiv}CR)_2]^+$ [8] and $[Pt_2(\mu\text{-dppm})_2(C{\equiv}CR)_4]$, first reported by Shaw, Pringle and coworkers [9,10]. It is believed that such systems, unlike the $[Pt_2(\mu\text{-dppm})_2(CN)_4]$ analogue [11,12], should offer a good opportunity for the systematic variation of the R substituents on the alkynyl group, which would provide insights for the understanding of the effect of the alkynyl ligand, in addition to the Pt···Pt interaction, on the spectroscopic properties of these complexes.

In this paper, the luminescence studies of two series of dinuclear platinum(II) complexes with the general formulae, $[Pt_2(\mu\text{-dppm})_2(\mu\text{-C}{\equiv}CR)(C{\equiv}CR)_2]^+$ and $[Pt_2(\mu\text{-dppm})_2(C{\equiv}CR)_4]$, are reported. Attempts have been made to correlate their luminescence properties to the variation of the alkynyl groups and the Pt···Pt contacts. Variable-temperature ^{1}H- and ^{31}P-NMR, and resonance Raman (RR) spectroscopic studies of $[Pt_2(\mu\text{-dppm})_2(\mu\text{-C}{\equiv}CPh)(C{\equiv}CPh)_2]^+$ have also been made. The syntheses of two mixed-metal complexes, $[Pt_2(\mu\text{-dppm})_2(C{\equiv}CPh)_4\cdot\{Cu(MeCN)\}_2]^{2+}$ and $[Pt_2(\mu\text{-dppm})_2(C{\equiv}CPh)_4\cdot\{Ag(MeCN)\}_2]^{2+}$, through the π-coordination of copper(I) or silver(I) ions in between the two alkynyl groups of $[Pt_2(\mu\text{-dppm})_2(C{\equiv}CPh)_4]$ have been accomplished and their luminescence properties determined.

2. A-frame dinuclear platinum(II) alkynyl complexes

2.1. Syntheses and characterization

The preparation of the first A-frame dinuclear platinum(II) alkynyl complex, $[Pt_2(\mu\text{-dppm})_2(\mu\text{-C}{\equiv}C^tBu)(C{\equiv}C^tBu)_2]^+$, was reported by Pringle and coworkers [8] by the reaction of $[Pt(dppm)Cl_2]$ with $LiC{\equiv}C^tBu$ in THF solution. Reaction using other alkynyllithium reagents ($LiC{\equiv}CPh$ or $LiC{\equiv}CC_6H_4\text{–Me-}p$) under similar conditions did not afford the desired A-frame complexes but instead yielded the face-to-face $[Pt_2(\mu\text{-dppm})_2(C{\equiv}CR)_4]$ complexes. We recently reported another synthetic route that could be employed as a more general synthetic methodology for the preparation of the A-frame complexes of arylacetylide, $[Pt_2(\mu\text{-dppm})_2(\mu\text{-C}{\equiv}CR)(C{\equiv}CR)_2]^+$ (R = C_6H_5, C_6H_4–OMe-p, C_6H_4–Et-p, C_6H_4–OEt-p, C_6H_4–^{n}Bu-p, C_6H_4–O^{n}Bu-p, C_6H_4–Ph-p) [13–17]. In this method, the organic alkyne was deprotonated by mercury(II) acetate to form the corresponding mercury acetylide in ethanol, which was then reacted with $[Pt(dppm)_2]Cl_2$ in refluxing ethanol to yield the A-frame product in reasonable yield (Scheme 1). The method employed is simple, direct, reliable and gives the desired product in fairly high yield when the alkynyl group used is arylacetylide. However, attempts to synthesize analogous complexes with alkyl acetylides of long hydrocarbon chain under the same reaction conditions only resulted in an interesting novel class of alkenylidene complexes [18].

These dinuclear A-frame platinum(II) alkynyl complexes show a regular A-frame structure with two terminal alkynyl groups and one bridgehead μ-η^1:η^2 alkynyl ligand, as revealed from their X-ray crystal structures. Each platinum atom exhibits a slightly distorted square-planar coordination which therefore results in an 'A-frame' type of structure and the methylene linkages of the dppm groups fold toward the apex of the 'A-frame'. The intramolecular Pt···Pt bond distances range from 2.903 to 3.236 Å, which are comparable to that found in other dinuclear platinum(II) complexes [3,11] and are indicative of the presence of Pt···Pt interactions. The Pt···Pt bond distance observed in $[Pt_2(\mu\text{-dppm})_2(\mu\text{-C}{\equiv}C\text{–}C_6H_4\text{–}^n\text{Bu-}p)(C{\equiv}C\text{–}C_6H_4\text{–}^n\text{Bu-}p)_2]^+$ (2.903 Å) [17] is surprisingly shorter than that for $[Pt_2(pop)_4]^{4-}$ (2.925(1) Å). For the μ_2-η^2-C≡C–C_6H_4–^{n}Bu-p group, the close resemblance of the two Pt–C≡C bond angles (1.382(6) and 135.4(6)°) as well as the almost identical Pt–C bond distances (1.121(9) and 1.121(8) Å) observed are indicative of a symmetrical alkynyl bridging mode. Such symmetrical bridging alkynyl group, which is nearly perpendicular to the Pt_2P_4 plane, makes the complex itself close to a regular A-frame structure and in a C_{2v} symmetry.

Two rather weak and ill-resolved IR bands in the 2000–2100 cm^{-1} region were observed in the IR

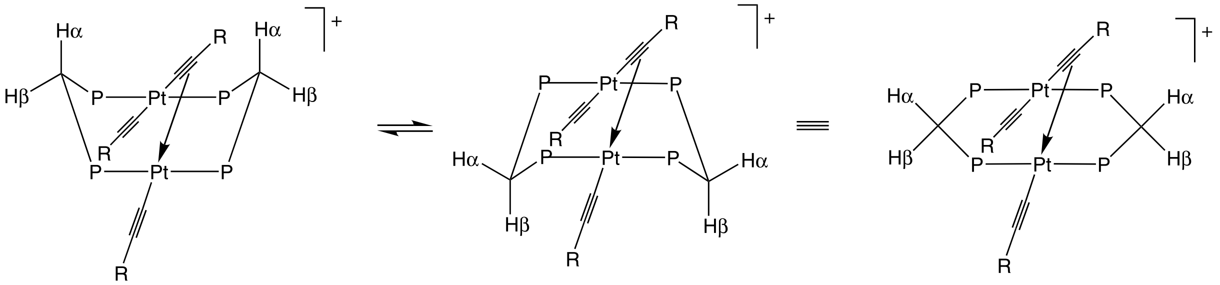

Scheme 2.

absorption spectra and were assigned as the ν(C≡C) stretches. The higher ν(C≡C) stretching frequency at ca. 2100 cm^{-1} is ascribed to the terminal alkynyl groups while the lower stretching frequency at ca. 2000 cm^{-1} to the μ-η^1:η^2 bridging alkynyl ligand. The lower stretching frequency for the μ-η^1:η^2 bridging alkynyl group is ascribed to the C≡C bond weakening as a result of π-donation to another platinum metal centre from the alkynyl group. It is interesting to note that three distinct ν(C≡C) stretches were observed in FT-Raman and RR spectra of $[Pt_2(\mu\text{-dppm})_2(\mu\text{-C≡CPh})(C≡CPh)_2]PF_6$, attributed to the three different alkynyl environments [14–16]. The observation of only two bands in the IR spectra may be due to the third band being too weak in intensity to be detectable or too close in frequency to the other two to be resolved.

In the room temperature ^{1}H-NMR spectra, two broad multiplets at ca. δ 4.5–5.0 ppm were observed for all the complexes and were assigned as the resonances of methylene protons of dppm ligand. In addition, two sets of hydrocarbon signals in the integral ratio of 2:1 have been observed for the complexes with alkyl- or alkoxyl-substituted phenylacetylides, suggestive of the presence of two non-equivalent alkynyl environments. Interestingly, similar ^{1}H-NMR spectroscopic results were observed even at −40 °C. According to these observations, two fluxional processes are proposed to occur. Although the structures of the A-frame complexes assumed a pseudo-boat conformation that was confirmed by X-ray crystallography, a time-averaged structure could be considered in which the $Pt_2P_4C_2$ unit appeared to assume a time-averaged co-planar arrangement through the inversion of the pseudo-boat or the so-called ‘flipping’ process (Scheme 2). At the same time, a σ,π-alkynyl exchange process or ‘windscreen wiper’ action (Scheme 3) would be expected to account for the equivalence of environment in the two terminal alkynyl groups. Similar σ,π-alkynyl exchange processes have been reported in other μ-alkynyl systems [8,19,20]. Such ‘windscreen wiper’ process could also account for the equivalence of both the ^{31}P and ^{195}Pt nuclei in the ^{31}P- and ^{195}Pt-NMR spectra of these A-frame complexes, in which a singlet at ca. δ 3.6 and a triplet signal at ca. δ −4600 ppm were observed, respectively. The observation of three non-equivalent alkynyl environments in the Raman spectra suggested that the rate of the σ,π-alkynyl exchange that led to the equivalence of the two terminal alkynyls, was fast on the NMR time-scale (ca. 10^{-2}–10^{-5} s) but much slower than the vibrational time-scale (ca. 10^{-12}–10^{-13} s). Upon raising the temperature to above room temperature, the two broad signals corresponding to the methylene protons in dppm as well as the alkyl- or alkoxyl-signals in the alkyl- or alkoxy-arylacetylide complexes eventually coalesced to a single signal, corresponding to the fluxional process associated with a bridging-to-terminal alkynyl ligand exchange (Scheme 4).

2.2. Electronic absorption and emission spectroscopy

All the A-frame dinuclear platinum(II) alkynyl complexes exhibit a low-energy absorption at ca. 400 nm with a shoulder at ca. 450 nm in acetonitrile or dichloromethane, that has been red-shifted with respect to the related mononuclear species, *trans*-$[Pt(\text{dppm-}P)_2(C≡CR)_2]$ [13,21], which shows an absorption band at ca. 345 nm in dichloromethane and was assigned as a metal-to-ligand charge transfer (MLCT) [d(Pt)→π*(C≡

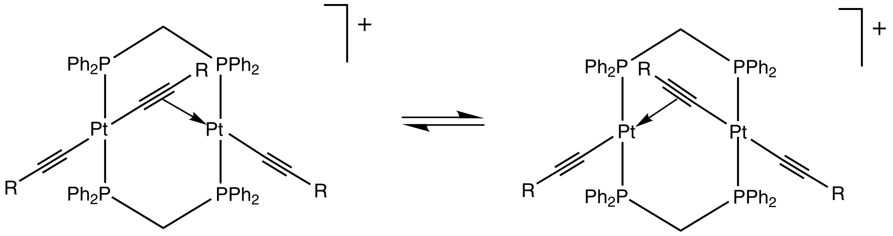

Scheme 3.

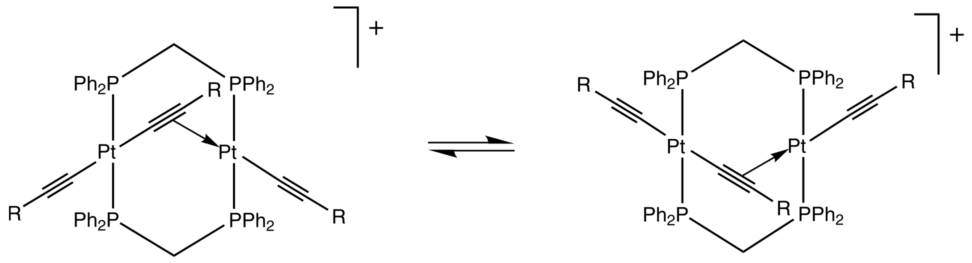

Scheme 4.

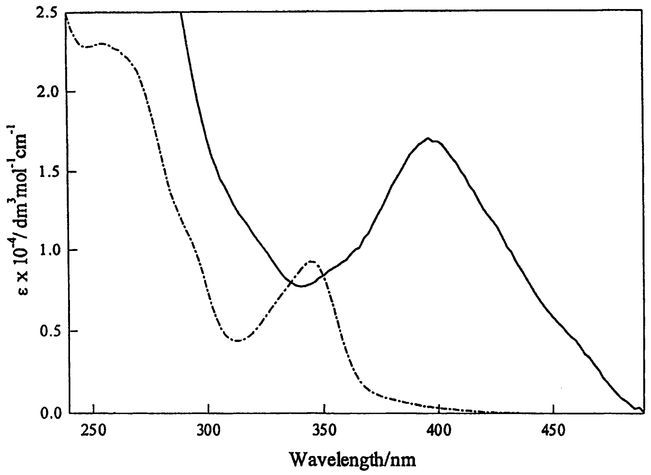

Fig. 1. Electronic absorption spectra of [Pt$_2$(μ-dppm)$_2$(μ-C≡CPh)(C≡CPh)$_2$]ClO$_4$ (—) and *trans*-[Pt(dppm-*P*)$_2$(C≡CPh)$_2$] (–·–·–) in CH$_2$Cl$_2$ at 298 K.

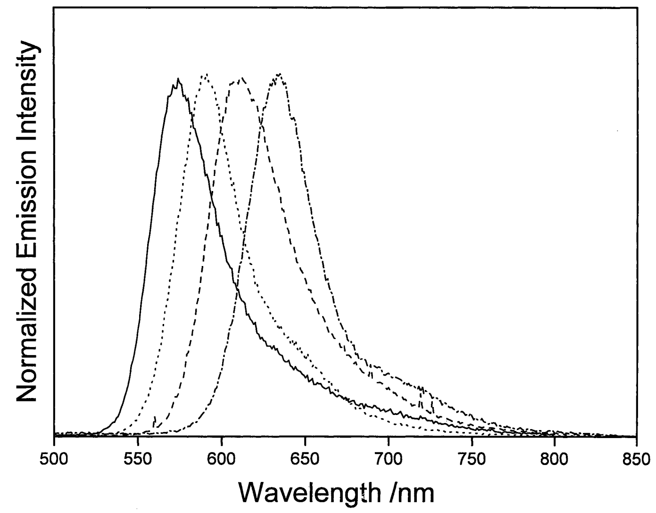

Fig. 2. The solid state emission spectra of [Pt$_2$(μ-dppm)$_2$(μ-C≡CC$_6$H$_4$–O^{n}Bu-*p*)(C≡CC$_6$H$_4$–O^{n}Bu-*p*)$_2$]ClO$_4$ (—), [Pt$_2$(μ-dppm)$_2$(μ-C≡CC$_6$H$_4$–Et-*p*)(C≡CC$_6$H$_4$–Et-*p*)$_2$]ClO$_4$ (···), [Pt$_2$(μ-dppm)$_2$(μ-C≡CC$_6$H$_4$–OMe-*p*)(C≡CC$_6$H$_4$–OMe-*p*)$_2$]ClO$_4$ (– – –) and [Pt$_2$(μ-dppm)$_2$(μ-C≡CC$_6$H$_4$–Ph-*p*)(C≡CC$_6$H$_4$–Ph-*p*)$_2$]ClO$_4$ (–·–·–) at room temperature.

CR)] transition. Fig. 1 shows the electronic absorption spectra of *trans*-[Pt(dppm-*P*)$_2$(C≡CPh)$_2$] and [Pt$_2$(μ-dppm)$_2$(μ-C≡CPh)(C≡CPh)$_2$]ClO$_4$ in dichloromethane. With reference to the previous spectroscopic work on dinuclear d^8–d^8 systems [11,12,22,23], the low-energy absorption bands observed in these A-frame complexes, which have been red-shifted with respect to the mononuclear analogues, have been assigned as a metal–metal bond-to-ligand charge transfer (MMLCT) [d$_\sigma^*$(Pt$_2$) → p$_\sigma$(Pt$_2$)/π*(C≡CR)] transition. The LUMO was believed to have substantial mixing of the π* of alkynyl group with the p$_\sigma$(Pt$_2$) orbital of the Pt–Pt bonding interaction, where d$_\sigma^*$ and p$_\sigma$ denote the antibonding combination of d$_{z^2}$(Pt)−d$_{z^2}$(Pt) interaction and bonding combination of p$_z$(Pt)–p$_z$(Pt) interaction, respectively, assuming a C_{2v} symmetry and taking Pt···Pt direction

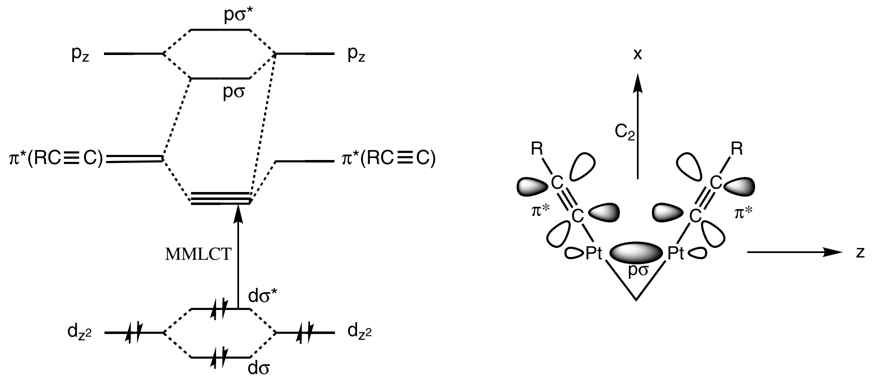

Scheme 5.

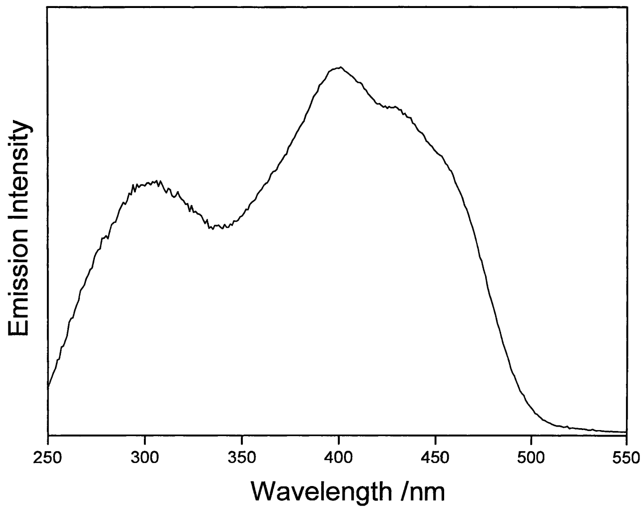

Fig. 3. The excitation spectrum of $[Pt_2(\mu\text{-dppm})_2(\mu\text{-}C{\equiv}CC_6H_4\text{–}{}^{n}Bu\text{-}p)(C{\equiv}CC_6H_4\text{–}{}^{n}Bu\text{-}p)_2]ClO_4$ monitored at 620 nm in degassed CH_3CN at room temperature.

as the z-axis (Scheme 5). The involvement of the $\pi^*(C{\equiv}CR)$ in the LUMO of these complexes has further been supported by the dependence of the absorption energy on the nature of the alkynyl ligands. For example, the absorption shoulder of $[Pt_2(\mu\text{-dppm})_2(\mu\text{-}C{\equiv}C^{t}Bu)(C{\equiv}C^{t}Bu)_2]^+$ (410 nm) in acetonitrile occurs at higher energy than that of $[Pt_2(\mu\text{-dppm})_2(\mu\text{-}C{\equiv}CPh)(C{\equiv}CPh)_2]^+$ (450 nm), consistent with a MMLCT assignment.

Upon photo-excitation at $\lambda > 350$ nm, the solid samples and fluid solutions of the complexes exhibit intense long-lived luminescence at room temperature. All the complexes exhibit a broad emission band at ca. 570–640 nm, attributed to phosphorescence with emission lifetimes in the microsecond range. The solid state emission energies of the complexes at room temperature, $[Pt_2(\mu\text{-dppm})_2(\mu\text{-}C{\equiv}CR)(C{\equiv}CR)_2]^+$, were found to depend on the nature of the alkynyl ligands, with an order of $R = {}^{t}Bu$ (554 nm) > $C_6H_4\text{–}O^{n}Bu\text{-}p$ (574 nm) > $C_6H_4\text{–}Et\text{-}p$ (590 nm) > $C_6H_4\text{–}OEt\text{-}p$ (595 nm) ≈ $C_6H_4\text{–}{}^{n}Bu\text{-}p$ (600 nm) > $C_6H_4\text{–}OMe\text{-}p$ (610 nm) > C_6H_5 (618 nm) > $C_6H_4\text{–}Ph\text{-}p$ (635 nm) in line with the decrease in the $\pi^*(C{\equiv}CR)$ orbital energy of the alkynyl ligand and is suggestive of the involvement of the alkynyl group in the transition. The solid-state emission spectra of selected complexes are depicted in Fig. 2. The resemblance of excitation maxima shown in the excitation spectra monitored at the emission maxima with the absorption maxima of the corresponding complexes suggests that the emissive state is probably due to a MMLCT origin. Fig. 3 shows the excitation spectrum of $[Pt_2(\mu\text{-dppm})_2(\mu\text{-}C{\equiv}CC_6H_4\text{–}{}^{n}Bu\text{-}p)(C{\equiv}CC_6H_4\text{–}{}^{n}Bu\text{-}p)_2]ClO_4$ monitored at 620 nm in degassed CH_3CN at room temperature. The two excitation bands at $\lambda > 400$ nm are tentatively assigned as the ${}^1[(d_\sigma^*)^2] \rightarrow {}^1[(d_\sigma^*)^1(p_\sigma/\pi^*)^1]$ (singlet–singlet) and ${}^1[(d_\sigma^*)^2] \rightarrow {}^3[(d_\sigma^*)^1(p_\sigma/\pi^*)^1]$ (singlet–triplet) transitions, respectively. Vibronic-structured bands with progressional spacings of ca. 2000 cm^{-1}, typically of the $\nu(C{\equiv}C)$ stretch in the ground state, were observed in the 77 K solid-state and EtOH/MeOH (4:1, v/v) glass emission spectra of the complexes, further supportive of the involvement of the alkynyl group in the emissive state. The solid-state emission spectra of $[Pt_2(\mu\text{-dppm})_2(\mu\text{-}C{\equiv}CC_6H_4\text{–}OEt\text{-}p)(C{\equiv}CC_6H_4\text{–}OEt\text{-}p)_2]ClO_4$ and $[Pt_2(\mu\text{-dppm})_2(\mu\text{-}C{\equiv}CC_6H_4\text{–}Ph\text{-}p)(C{\equiv}CC_6H_4\text{–}Ph\text{-}p)_2]ClO_4$ at 77 K are shown in Fig. 4. The possible assignment of an intraligand (IL) $\pi\text{–}\pi^*(C{\equiv}CR)$ origin would be less likely, given the relatively small Huang–Rhys factor ($S < 1$) observed from these spectra.

The phosphorescent states of these A-frame complexes were found to be quenched by pyridinium quenchers and the bimolecular quenching rate constants, kq, have been determined. In general, the more positive reduction potentials of the quenchers were, the higher would be the quenching rate constants found. An oxidative electron transfer mechanism has been suggested for the quenching reaction.

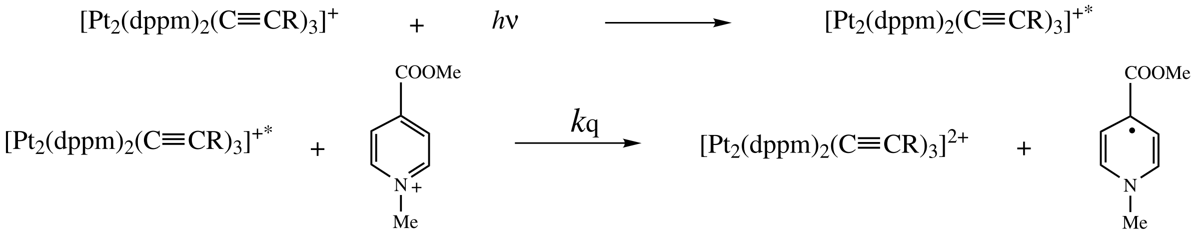

The transient absorption spectra show an absorption band at ca. 380–390 nm characteristic of the pyridinyl radicals, confirming the electron transfer nature of the

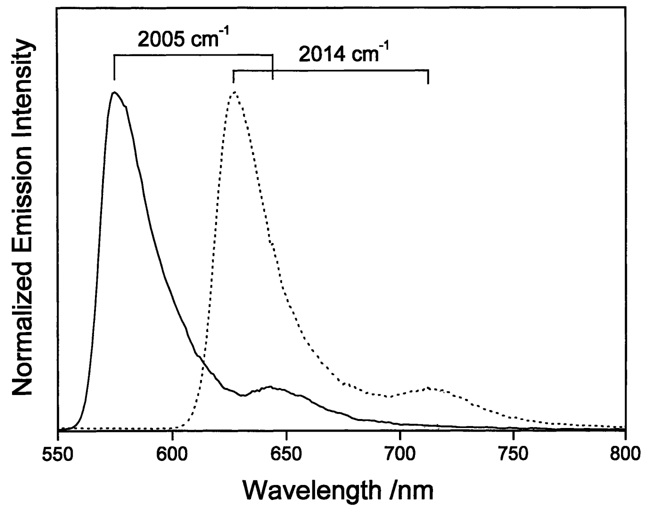

Fig. 4. The solid-state emission spectra of $[Pt_2(\mu\text{-dppm})_2(\mu\text{-C}{\equiv}CC_6H_4\text{–OEt-}p)(C{\equiv}CC_6H_4\text{–OEt-}p)_2]ClO_4$ (—) and $[Pt_2(\mu\text{-dppm})_2(\mu\text{-C}{\equiv}CC_6H_4\text{–Ph-}p)(C{\equiv}CC_6H_4\text{–Ph-}p)_2]ClO_4$ (···) at 77 K.

quenching reactions. Apart from the absorption band at ca. 380–390 nm which is typical of the pyridinyl radical and the bleaching at ca. 400 nm which somewhat obscures the pyridinyl radical absorption [24], an intense absorption difference band at ca. 510 nm with a shoulder at ca. 450 nm was observed. It is likely that the absorption bands at ca. 450–510 nm, which are not characteristic of the pyridinyl radical, are the result of the absorption of the one-electron oxidized form of the metal complex.

2.3. RR spectroscopy

In order to gain more insights into the spectroscopic origin of the transitions, RR experiments of $[Pt_2(\mu\text{-dppm})_2(\mu\text{-C}{\equiv}CPh)(C{\equiv}CPh)_2]^+$ and its related mononuclear analogue, *trans*-$[Pt(dppm\text{-}P)_2(C{\equiv}CPh)_2]$, have been carried out [14–16]. The RR spectrum of the mononuclear species shows only one intense C≡C stretch peak at ca. 2114 cm^{-1}. The relative intensity patterns for the RR spectra obtained with excitation (310 nm $< \lambda_{ex} <$ 370 nm) within the transition centred at ca. 345 nm are very similar to one another. These, together with the agreement of the absolute cross section measurements to the basic profile of the absorption spectra, suggest that the resonance enhancements of the ν(C≡C) stretch are due to the strong d(Pt) → π*(C≡CPh) MLCT transition band. The RR spectrum of $[Pt_2(\mu\text{-dppm})_2(\mu\text{-C}{\equiv}CPh)(C{\equiv}CPh)_2]^+$ displays three very strong C≡C stretching vibration peaks at 2027, 2062, and 2125 cm^{-1}, corresponding to the three different alkynyl ligand environments. The lowest frequency stretching vibration at 2027 cm^{-1} is assigned as the μ-bridging C≡C vibration while the other two are tentatively assigned as the terminal C≡C vibrations.

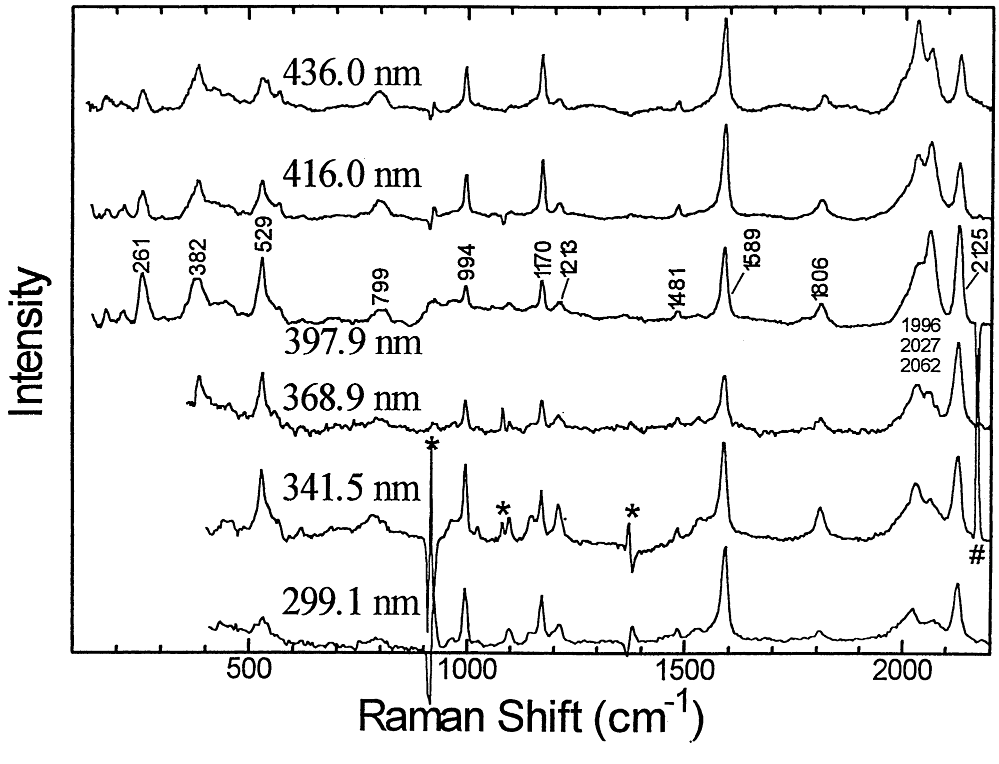

Fig. 5. Overview of the RR spectra of $[Pt_2(\mu\text{-dppm})_2(\mu\text{-C}{\equiv}CPh)(C{\equiv}CPh)_2]^+$ in acetonitrile solution.

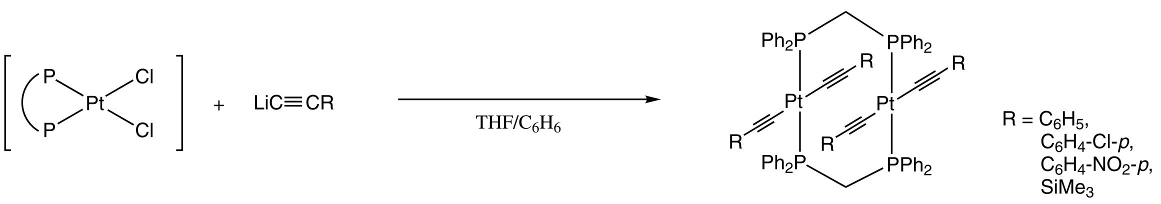

Scheme 6.

Similarly, the RR spectra (420 nm $< \lambda_{em} <$ 365 nm) receive most of their resonance enhancements from the intense $d_\sigma^*(Pt_2) \rightarrow p_\sigma(Pt_2)/\pi^*(C{\equiv}CPh)$ MMLCT transition centred at 393 nm. The intensity of the peak at 2125 cm^{-1} relative to the 2062 and 2027 cm^{-1} peaks is the highest upon excitation into the blue edge of the MMLCT absorption band and decreases as the excitation wavelength moves toward the red edge of the MMLCT band. Fig. 5 displays the overview of the RR spectra of $[Pt_2(\mu\text{-dppm})_2(\mu\text{-}C{\equiv}CPh)(C{\equiv}CPh)_2]^+$ in acetonitrile solution. Such observation is suggestive of the presence of more than one configuration attributable to the MMLCT absorption band as a result of photo-induced charge transfer to the different localized C≡C bonds, in which excitation to the red-edge of the MMLCT band would selectively excite the MMLCT transition that is more localized on the $\pi^*(\mu\text{-}C{\equiv}CPh)$ orbital and gave rise to preferential resonance enhancement of the 2027 cm^{-1} peak.

3. Face-to-face dinuclear platinum(II) alkynyl complexes and their mixed-metal copper(I) and silver(I) complexes

3.1. Syntheses and characterization

The face-to-face dinuclear platinum(II) alkynyl complex, $[Pt_2(\mu\text{-dppm})_2(C{\equiv}CPh)_4]$, was first synthesized by Shaw and coworkers [9,10]. In this method, reaction of freshly prepared lithium phenylacetylide with $[Pt(dppm)Cl_2]$ in THF–benzene under reflux condition afforded the desired complex. Employing the same synthetic methodology, a series of analogous complexes with various acetylides, $[Pt_2(\mu\text{-dppm})_2(C{\equiv}CR)_4]$ (R = C_6H_4–Cl-*p*, C_6H_4–NO_2-*p*, $SiMe_3$), has been prepared by us [25,26] (Scheme 6). All of them exist as air-stable pale yellow solids with the exception of the nitro-substituted analogue, which is an orange–yellow solid. In view of the numerous reports on the use of metal alkynyl systems as η^2-ligands to form tweezer-like/sandwich complexes [27–32] and the structure of the face-to-face complex showing two pairs of the alkynyl ligands that have been pre-organized for the ready encapsulation of other metal ions through π-coordination, attempts were made to employ them as precursors for the formation of mixed-metal complexes, in which the metal ions are sandwiched between the alkynyl groups within the same dinuclear face-to-face complex. By the reaction of $[Pt_2(\mu\text{-dppm})_2(C{\equiv}CPh)_4]$ and $[M(MeCN)_4]^+$ (M = Cu or Ag), two novel tetranuclear mixed-metal platinum(II)–copper(I) and –silver(I) complexes, $[Pt_2(\mu\text{-dppm})_2(C{\equiv}CPh)_4\cdot\{Cu(MeCN)\}_2](PF_6)_2$ and $[Pt_2(\mu\text{-dppm})_2(C{\equiv}CPh)_4\cdot\{Ag(MeCN)\}_2](BF_4)_2$, have been synthesized and isolated (Scheme 7). In contrast to the homometallic platinum(II) face-to-face complexes, which are only sparsely soluble in dichloromethane, the mixed-metal complexes have good solubilities in dichloromethane, acetone and acetonitrile.

All the face-to-face dinuclear platinum(II) alkynyl complexes have been structurally characterized by X-ray crystallography [25,26] and they show a face-to-face conformation. Each platinum atom exhibits a distorted square-planar geometry, with two alkynyl groups and two bridging dppm ligands coordinated in a *trans*

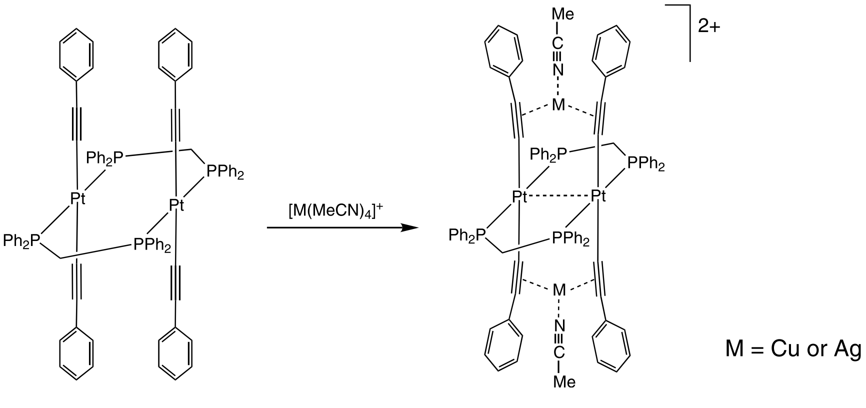

Scheme 7.

arrangement. The two platinum square planes are eclipsed with respect to each other and form an eight-membered ring with the bridging dppm ligands. Similar structural arrangement has been observed for the mixed-metal complexes, except that in addition, the two copper(I) or silver(I) metal ions are encapsulated by the two pairs of alkynyl groups and coordinated to one acetonitrile molecule in trigonal-planar geometry. The C≡C bond distances are in the range of 1.19–1.21 Å, typical of other C≡C bond distances in related platinum alkynyl systems [13,18,33–35]. In all cases, Pt···Pt interactions are present as revealed by their short Pt···Pt *Ptcontacts*(3.012{{\tf="BMa1"\-
(3.012–3.437 Å). It is interesting to note that the Pt···Pt distances in [Pt$_2$(μ-dppm)$_2$(C≡CR)$_4$] vary with the nature of the alkynyl ligands. In general, shorter Pt···Pt distances were found for complexes with less electron-rich alkynyl groups (R = Ph, 3.437 Å; C$_6$H$_4$–Cl-*p*, 3.430 Å; C$_6$H$_4$–NO$_2$-*p*, 3.250 Å; SiMe$_3$, 3.349 Å). The weaker donor strength of the less electron-rich alkynyl ligands, which would lead to a reduced electron density on the platinum centres, would tend to pull the metal centres closer for metal–metal interactions to occur.

The Pt···Pt distances in the mixed-metal complexes, [Pt$_2$(μ-dppm)$_2$(C≡CPh)$_4$·{M(MeCN)}$_2$]$^{2+}$ (M = Cu, 3.0124 Å; Ag, 3.064 Å), are even shorter than the precursor complex [Pt$_2$(μ-dppm)$_2$(C≡CPh)$_4$] (3.437 Å). This has been ascribed to the encapsulation of copper(I) or silver(I) metal ion by two adjacent alkynyl ligands, which pulls the platinum atoms into close proximity as a result of the reduced donor strength of the alkynyl ligands as well as the steric demands required upon copper(I) or silver(I) coordination.

3.2. Electronic absorption and emission spectroscopy

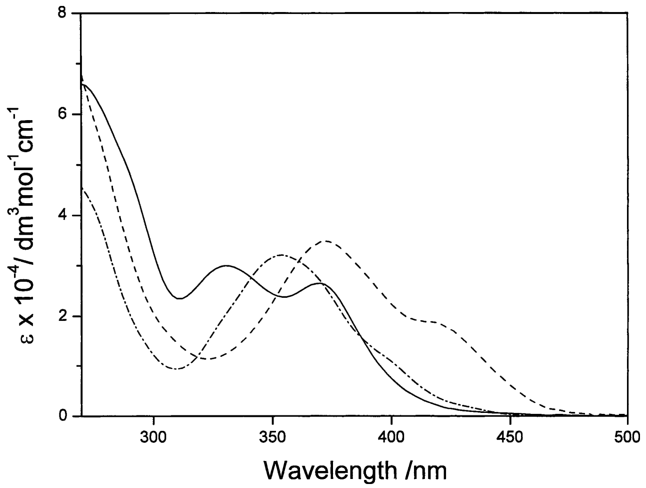

Fig. 6. The electronic absorption spectra of [Pt$_2$(μ-dppm)$_2$(C≡CPh)$_4$] (—), [Pt$_2$(μ-dppm)$_2$(C≡CPh)$_4$·{Cu(MeCN)}$_2$]$^{2+}$ (– – –) and [Pt$_2$(μ-dppm)$_2$(C≡CPh)$_4$·{Ag(MeCN)}$_2$]$^{2+}$ (–·–·–) in dichloromethane at room temperature.

The electronic absorption spectra of the face-to-face complexes and their mixed-metal complexes show two low-energy absorption bands at ca. 318–386 and 372–418 nm in dichloromethane solution. The position of these low-energy absorption bands depends on the nature of the alkynyl ligands and the coordination of d^{10} metal centres. In general, the mixed-metal complexes absorb at lower energy than their face-to-face precursors. With reference to the spectroscopic studies on the related mononuclear *trans*-[Pt(dppm-P)$_2$(C≡CR)$_2$], which absorbs at ca. 345 nm due to a metal-to-ligand charge transfer (MLCT) [d(Pt) → π*(C≡CR)] transition, the low-energy absorptions in the face-to-face complexes and their mixed-metal counterparts, similar to that of the A-frame system, are suggested to involve a transition of substantial MMLCT ^{1}[d$_{\sigma}^{*}$(Pt$_2$) → p$_{\sigma}$(Pt$_2$)/π*(C≡CR)] character (Scheme 8). This has been substantiated by the energy dependence of the low-energy absorption on the π*(C≡CR) orbital energy. For example, the lowest-energy absorption of [Pt$_2$(μ-dppm)$_2$(C≡CC$_6$H$_4$–NO$_2$-*p*)$_4$] occurs at 415 nm, which is at lower energy than that of [Pt$_2$(μ-dppm)$_2$(C≡CPh)$_4$] which occurs at 370 nm. Fig. 6 depicts the electronic absorption spectra of selected complexes. Similar assignments have also

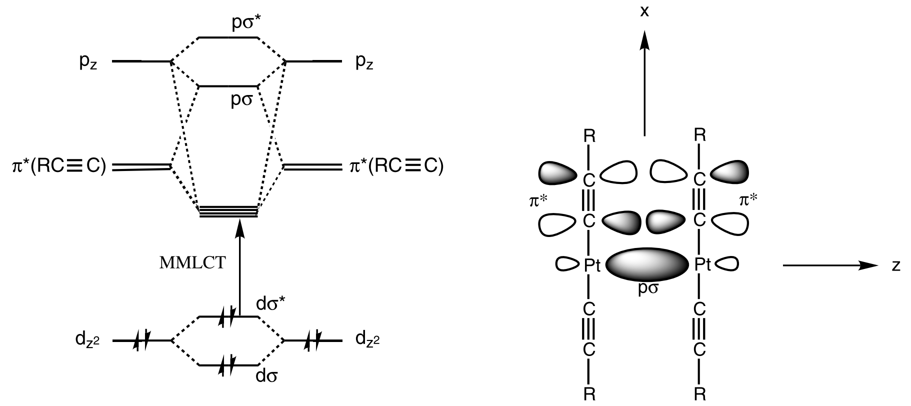

Scheme 8.

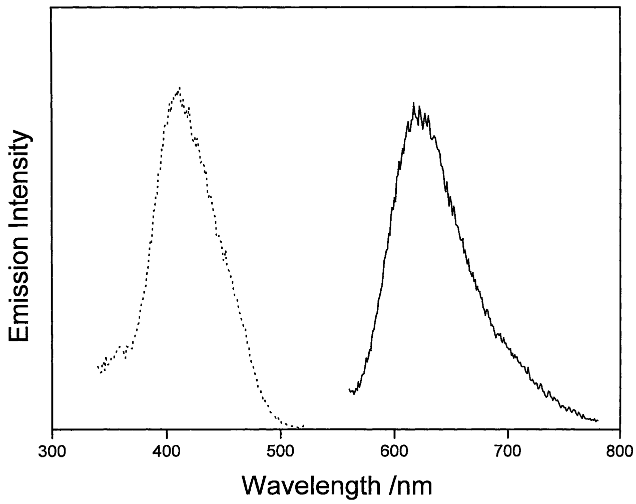

Fig. 7. The emission (—) and excitation (···) spectra of [Pt_2(μ-dppm)$_2$(C≡CPh)$_4$] in dichloromethane.

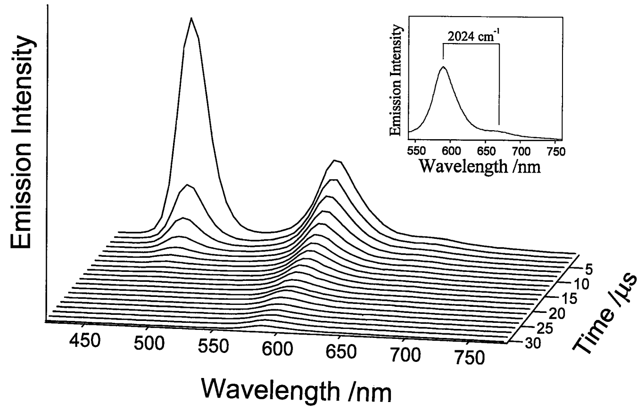

Fig. 8. The 3D-plot of the time-resolved emission spectra of [Pt_2(μ-dppm)$_2$(C≡CPh)$_4$·{Cu(MeCN)}$_2$](PF$_6$)$_2$ in EtOH/MeOH glass (4:1 v/v) at 77 K.

been suggested for [Pt_2(dppm)$_2$(CN)$_4$] [11], [Rh_2(dppm)$_2$(CNR)$_4$] [22] and the binuclear Pt(II) μ-alkenylidene complexes [18,23]. On the other hand, the low-energy electronic absorptions for the mixed-metal complexes, [Pt_2(μ-dppm)$_2$(C≡CPh)$_4$·{M(MeCN)}$_2$]$^{2+}$ (M = Cu, 418 nm; Ag, 400 nm) are red-shifted with respect to their precursor complex, [Pt_2(μ-dppm)$_2$(C≡CPh)$_4$] (370 nm). Encapsulation of copper(I) or silver(I) metal ions would result in the raising of the $d_{\sigma}^{*}(Pt_2)$ orbital energy (HOMO) due to the shortening of the Pt···Pt distance and a lowering of the $p_{\sigma}(Pt_2)/\pi^{*}$(C≡CPh) orbital energy (LUMO) as a result of an increase in the alkynyl π-acceptor ability upon π-donation to copper(I) or silver(I). Both of these effects would cause a narrowing of the HOMO–LUMO energy gap for this MMLCT transition and account for the red-shift of the absorption band.

Upon excitation at $\lambda > 350$ nm, the face-to-face and mixed-metal complexes exhibit strong luminescence in the solid-state and in fluid solution at room temperature and 77 K. The emission spectra in dichloromethane show an emission band at ca. 620–664 nm. With reference to previous spectroscopic works on related d^8–d^8 dinuclear systems [11–13,16,23] and the close resemblance of the excitation maxima to the low-energy absorptions, the emission band is ascribed to phosphorescence derived from the ^{3}MMLCT state. The excitation and emission spectra of [Pt_2(μ-dppm)$_2$(C≡CPh)$_4$] in dichloromethane are shown in Fig. 7. Similar to the electronic absorption, the emission of [Pt_2(μ-dppm)$_2$(C≡CC$_6$H$_4$–NO$_2$-*p*)$_4$] (664 nm) occurs at lower energy than that of [Pt_2(μ-dppm)$_2$(C≡CPh)$_4$] (620 nm). The red-shift of the ^{3}MMLCT emission energy of the nitrophenyl analogue relative to that of the phenylacetylide complex is ascribed to the lower π*(C≡CC$_6$H$_4$–NO$_2$-*p*) orbital energy in the presence of the electron-withdrawing nitro substituent. In the solid-state and glass state at 77 K, the emission spectra exhibit two emission bands at ca. 460–500 and 545–634 nm. Fig. 8 displays the 3D-plot of the time-resolved emission spectra of [Pt_2(μ-dppm)$_2$(C≡CPh)$_4$·{Cu(MeCN)}$_2$](PF$_6$)$_2$ in EtOH/MeOH glass (4:1 v/v) at 77 K. In view of their large energy separation and difference in excited-state lifetimes, they are suggested to be of different origins. The higher energy emission was tentatively assigned as IL phosphorescence. The lower energy vibronic-structured emission, with vibrational progressional spacings of ca. 2000–2200 cm^{-1} that is typical of the ν(C≡C) stretch in the ground state, is suggestive of an involvement of the C≡CR moiety in the emissive state, and is most probably derived from the ^{3}MMLCT state. The lower emission energy of the mixed-metal complexes than the precursor complex in 77 K glass is consistent with this ^{3}MMLCT assignment as a result of the narrowing of the HOMO–LUMO energy gap upon metal ion π-coordination.

4. Concluding remarks

This review summarizes the photophysical studies of two classes of dinuclear platinum(II) alkynyl complexes, the A-frame [Pt_2(μ-dppm)$_2$(μ-C≡CR)(C≡CR)$_2$]$^+$ and the face-to-face [Pt_2(μ-dppm)$_2$(C≡CR)$_4$] together with their mixed-metal complexes, [Pt_2(μ-dppm)$_2$(C≡CPh)$_4$·{Cu(MeCN)}$_2$]$^{2+}$ and [Pt_2(μ-dppm)$_2$(C≡CPh)$_4$·{Ag(MeCN)}$_2$]$^{2+}$. All the complexes exhibit strong luminescence upon photo-excitation, assigned as derived from states of a triplet metal–metal bond-to-ligand charge transfer (^{3}MMLCT) [$d_{\sigma}^{*}(Pt_2) \rightarrow p_{\sigma}(Pt_2)/\pi^{*}$(C≡CR)] origin. By using different alkynyl groups, the ^{3}MMLCT emission energy can be fine-tuned due to the variation of π*(C≡CR) orbital energy as well as the $d_{\sigma}^{*}(Pt_2)$ orbital energy resulted from a variation in the Pt···Pt distances. In general, lower emission energy was observed in the A-frame system relative to the face-to-face system due to the presence of the lower-lying $\pi^*(C\equiv CR)$ orbital of the bridging alkynyl group, μ-C≡CR. RR spectroscopic studies supported the involvement of the C≡CR group in the electronic transition and hence the assignment of the ^{3}MMLCT emission origin. Encapsulation of copper(I) or silver(I) metal ions in the mixed-metal complexes led to a red-shift of the MMLCT absorption and ^{3}MMLCT emission bands compared to that of the precursor. Such a phenomenon has been ascribed to the narrower HOMO–LUMO energy separation by the raising of the $d^*_\sigma(Pt_2)$ orbital and the lowering of the $\pi^*(C\equiv CR)$ orbital energy upon coordination of d^{10} metal ions by the alkynyl groups.

Acknowledgements

V.W.-W.Y. acknowledges support from The University of Hong Kong, and the receipt of a Croucher Senior Research Fellowship (2000–2001) from the Croucher Foundation; K.M.-C.W. the receipt of a University Postdoctoral Fellowship, and C.-K.H. and K.-L.Y. the receipt of postgraduate studentships administered by The University of Hong Kong. The work described in this paper has been fully supported by a grant from the Research Grants Council of the Hong Kong Special Administrative Region, China (Project No. HKU 7123/00P).

References

[1] R.S. Osborn, D. Rogers, J. Chem. Soc. Dalton Trans. (1974) 1002.
[2] R.H. Herber, M. Croft, M.J. Coyer, B. Bilash, A. Sahiner, Inorg. Chem. 33 (1994) 2422.
[3] D.M. Roundhill, H.B. Gray, C.M. Che, Acc. Chem. Res. 22 (1989) 55.
[4] V.W.W. Yam, J. Photochem. Photobiol. A 106 (1997) 75.
[5] V.W.W. Yam, K.K.W. Lo, Chem. Soc. Rev. 28 (1998) 323.
[6] V.W.W. Yam, K.K.W. Lo, K.M.C. Wong, J. Organomet. Chem. 587 (1998) 3.
[7] V.W.W. Yam, Chem. Commum. (2001) 789.
[8] N.W. Alcock, T.J. Kemp, P.G. Pringle, P. Bergamini, O. Traverso, J. Chem. Soc. Dalton Trans. (1987) 1659.
[9] P.G. Pringle, B.L. Shaw, J. Chem. Soc. Chem. Commun. (1982) 581.
[10] C.R. Langrich, D.M. McEwan, P.G. Pringle, B.L. Shaw, J. Chem. Soc. Dalton Trans. (1983) 2487.
[11] C.M. Che, V.W.W. Yam, W.T. Wong, T.F. Lai, Inorg. Chem. 28 (1989) 2908.
[12] H.K. Yip, H.M. Lin, K.K. Cheung, C.M. Che, Y. Wang, Inorg. Chem. 33 (1994) 1644.
[13] V.W.W. Yam, L.P. Chan, T.F. Lai, Organometallics 12 (1993) 2197.
[14] W.M. Kwok, D.L. Phillips, P.K.Y. Yeung, V.W.W. Yam, Chem. Phys. Lett. 262 (1996) 699.
[15] W.M. Kwok, D.L. Phillips, P.K.Y. Yeung, V.W.W. Yam, J. Phys. Chem. Sect. A 101 (1997) 9286.
[16] V.W.W. Yam, P.K.Y. Yeung, L.P. Chan, W.M. Kwok, D.L. Phillips, K.L. Yu, R.W.K. Wong, H. Yan, Q.J. Meng, Organometallics 17 (1998) 2590.
[17] V.W.W. Yam, K.L. Yu, K.K. Cheung, unpublished results.
[18] V.W.W. Yam, K.L. Yu, B.W.K. Chu, K.K. Cheung, Organometallics 20 (2001) 3632.
[19] A.A. Cherkas, L.H. Randall, S.A. MacLaughlin, G.N. Mott, N.J. Taylor, A.J. Carty, Organometallics 7 (1988) 969.
[20] S. Top, M. Gunn, G. Jaouen, J. Vaissermann, J.C. Daran, M.J. McGlinchey, Organometallics 11 (1992) 1201.
[21] H. Masai, K. Sonogashira, N. Hagihara, Bull. Chem. Soc. Jpn. 44 (1971) 2226.
[22] K.R. Mann, J.G. Gordon, II, H.B. Gray, J. Am. Chem. Soc. 97 (1975) 3553.
[23] L.A. Sacksteder, E. Baralt, B.A. DeGraff, C.M. Lukehart, J.M. Demas, Inorg. Chem. 30 (1991) 3955.
[24] J. Hermolin, M. Levin, E.M. Kosower, J. Am. Chem. Soc. 103 (1981) 4808.
[25] V.W.W. Yam, K.L. Yu, K.M.C. Wong, K.K. Cheung, Organometallics 20 (2001) 721.
[26] V.W.W. Yam, C.K. Hui, K.M.C. Wong, N. Zhu, K.K. Cheung, submitted for publication.
[27] R. Nast, Coord. Chem. Rev. 47 (1982) 89.
[28] W. Beck, B. Niemer, M. Wieser, Angew. Chem. Int. Ed. Engl. 32 (1993) 923.
[29] H. Lang, K. Köhler, S. Blau, Coord. Chem. Rev. 143 (1995) 113.
[30] J. Forniés, E. Lalinde, J. Chem. Soc. Dalton Trans. (1996) 2587.
[31] V.W.W. Yam, K.L. Yu, K.K. Cheung, J. Chem. Soc. Dalton Trans. (1999) 2913.
[32] V.W.W. Yam, S.H.F. Chong, K.M.C. Wong, K.K. Cheung, Chem. Commun. (1999) 1013.
[33] V.W.W. Yam, R.P.L. Tang, K.M.C. Wong, K.K. Cheung, Organometallics 20 (2001) 4476.
[34] S. Leininger, P.J. Stang, S. Huang, Organometallics 17 (1998) 3981.
[35] K. Onitsuka, M. Fujimoto, N. Ohshiro, S. Takahashi, Angew. Chem. Int. Ed. Engl. 38 (1999) 689.